

## Room Temperature Resonant-Tunneling Hot Electron Transistors with dc and Microwave Gain

Alan SEABAUGH, Yung-Chung KAO, John RANDALL, William FRENSLEY, and  
Ali KHATIBZADEH

Central Research Laboratories  
Texas Instruments Incorporated  
Dallas, TX 75265

Room temperature operation is achieved in In(GaAl)As/InGaAs resonant-tunneling hot electron transistors (RHET) grown by molecular beam epitaxy on InP substrates. RHETs with base widths of 10, 40 and 60 nm were fabricated and all exhibit room temperature dc current gain greater than 2, with gain as high as 12 observed at resonance in the 40 nm base device. To our knowledge these are the first In(GaAl)As hot electron transistors to exhibit 300 K dc gain of this magnitude. S-parameter measurements of the 40(60) nm base RHET give values for  $f_T$  and  $f_{MAX}$  of 67(54) and 41(11) GHz, respectively.

### 1. INTRODUCTION

Resonant-tunneling hot electron transistors (RHET) have been demonstrated with 77 K common emitter current gain, on both GaAs and InP substrates<sup>1)</sup>. Recently, gain as high as 2.5 has been achieved in an InP-based RHET<sup>2)</sup>. To our knowledge, the sole other HET to operate with current gain at room temperature was fabricated using AlGaAsSb heterojunctions<sup>3)</sup>. We report here the dc and microwave characterization of InP-based RHETs with room temperature gain as high as 12.

### 2. DEVICE STRUCTURE

In the RHET, the resonant tunneling diode injector is used to direct a quasi-monoenergetic electron beam into the base. The base injection energy is chosen to be less than the L and X intervalley transfer energies (to minimize intervalley scattering), but greater than the base/collector barrier,  $\phi_{BC}$ . To achieve this condition one must use thin tunnel barriers and spacer layers to minimize the voltage drop across the injector. Even with thin tunnel

barriers and spacer layers, a simple RTD injector (such as AlAs/In<sub>0.53</sub>Ga<sub>0.47</sub>As/AlAs) has a base injection energy significantly above  $\phi_{BC}$ . The RTD well width can be increased to energetically lower the n=1 resonance thus lowering the injection energy, however this results in an undesirable decrease in peak-current density,  $J_p$ , and peak-to-valley current-ratio (PVR).

An alternative way to reduce the n=1 state energy is to incorporate a low bandgap layer within the quantum well as has recently been demonstrated by Broekaert, et al.<sup>4)</sup>. Using an RTD injector with an InAs notch in the center of the quantum well, a low base injection energy can be achieved while still maintaining high PVR and  $J_p$ .

The calculated energy band profile for a RHET using a notched RTD injector is shown in Fig.1 for the 40 nm base device described here. The profile is obtained from a self-consistent zero-current solution of Poisson's equation<sup>5)</sup>. Transmission resonances are computed self-consistently from the potential profile.

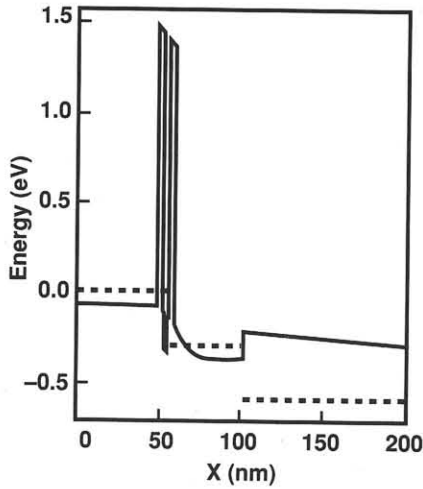


Fig.1 Calculated potential profile vs position, X, for the 40 nm base RHET. The dashed lines indicate the quasi-Fermi levels in the emitter, base, and collector for  $V_{BE}=0.3$  V and  $V_{CB}=0.3$  V

The materials were grown in a Riber 2300 MBE with the following structure, Table 1.

layer	semiconductor	nm	$\text{cm}^{-3}$
emitter cap	$\text{In}_{0.53}\text{Ga}_{0.47}\text{As}$	300	$1 \times 10^{19}$
emitter	$\text{n}^+\text{In}_{0.53}\text{Ga}_{0.47}\text{As}$	50	$1 \times 10^{18}$
spacer	$\text{In}_{0.53}\text{Ga}_{0.47}\text{As}$	1.5	undoped
barrier	AlAs	2	undoped
well	$\text{In}_{0.53}\text{Ga}_{0.47}\text{As}$	1	undoped
notch	InAs	2	undoped
well	$\text{In}_{0.53}\text{Ga}_{0.47}\text{As}$	1	undoped
barrier	AlAs	2	undoped
spacer	$\text{In}_{0.53}\text{Ga}_{0.47}\text{As}$	1.5	undoped
base	$\text{n}^+\text{In}_{0.53}\text{Ga}_{0.47}\text{As}$	t	$1 \times 10^{18}$
collector	$\text{In}_{0.5}(\text{Al}_{0.5}\text{Ga}_{0.5})\text{As}$	300	undoped
graded layer		50	undoped
subcollect.	$\text{n}^+\text{In}_{0.53}\text{Ga}_{0.47}\text{As}$	550	$5 \times 10^{18}$
substrate	InP Fe-doped		

Table 1. MBE layer diagram. A set of three devices with different base widths was grown,  $t=10, 40,$  and  $60$  nm. Back-ground doping in the InGaAs is typically  $2 \times 10^{15} \text{ cm}^{-3}$ .

In addition to serving as an injector, the RTD is used as a process monitor to indicate when the quantum well base etching is completed. The devices described here were fabricated using conventional wet-chemical etching techniques, mesa isolation, nonalloyed contacts, and air-bridge interconnects.

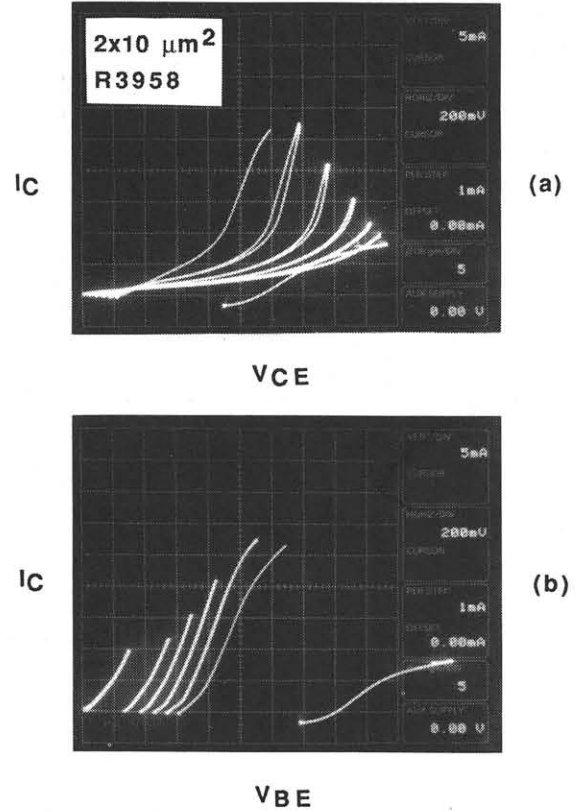


Fig.2 Room temperature common-emitter transistor characteristics for the 40 nm base RHET: (a)  $I_C$  vs  $V_{CE}$  for  $I_B=0,1,2,3,4,5$  mA and (b)  $I_C$  vs  $V_{BE}$  for the same set of base current steps. Zero collector current is offset one division.

### 3. DC CHARACTERISTICS

Room temperature gain was achieved in all three of the RHETs: 10 nm, 40 nm, and 60 nm base width. Common emitter transistor characteristics of the 40 nm device for five base current steps are shown in Fig.2. Collector/base leakage gives rise to the nonzero collector current,  $I_C$ , for the first base current step, corresponding to  $I_B=0$ . For the fifth base current step,  $I_B=5$  mA, the collector current is discontinuous at  $V_{CE}=1.2$  V where the injector RTD passes through resonance. Gain at resonance in this device exceeds 12 at a current density of  $2.6 \times 10^4 \text{ A/cm}^2$ .

At  $V_{BE}=1.3$  V the injector RTD is switched out of resonance (Fig.2b). When this occurs the base/emitter voltage,  $V_{BE}$ ,

increases causing the collector/base junction to switch to a weak forward bias. This manifests itself as a negative collector current in the off-resonance condition and is seen in both Figs.2(a) and (b). The collector current switches from a value of 5.3 mA at  $V_{CE}=1.2$  V to  $-0.3$  mA at  $V_{CE}=0.9$  V due to this forward-biasing of the collector/base junction. The switching of  $V_{CE}$  is a dynamic effect associated with charging of the RTD injector during the curve tracer (Tektronix 370) measurement and is not observed in ramped dc measurements (see Fig.3). At the resonance peak, the collector base voltage,  $V_{CB}$ , is nearly zero, therefore the current gain is not due to carrier multiplication in the base/collector junction.

Collector/base leakage gives rise to the nonzero collector current seen most readily for the zero base current step. Cooling the device to 77 K does not eliminate the leakage, however on cooling to 4.2 K, the leakage is significantly reduced. This suggests that the unintentional background doping density in the In(AlGa)As collector freezes out below 77 K. Shown in Fig.3 is the common-emitter transistor characteristic for another 40 nm RHET at 4.2 K, showing also the base/emitter voltage dependence on  $V_{CE}$ . A sharp increase in the conductance is observed at  $V_{CE}=340$  meV for  $I_B=800$   $\mu$ A. This is explained by the energetic alignment of a resonant state within the quantum well base itself.

It is possible to measure these transmission resonances through the quantum well by fixing the collector/base voltage and measuring the input conductance,  $dI_E/dV_{BE}$ , as a function of  $V_{BE}$ <sup>6)</sup>. Enhanced conductance occurs when the injected emitter electrons align with quantum well resonant states. This measurement is shown in Fig.4 where collector current and device input

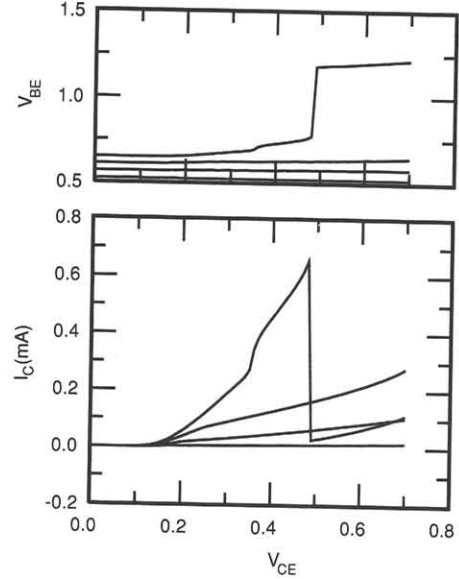


Fig.3 Common-emitter characteristics at 4.2 K for the 40 nm base RHET. The emitter area is circular with an area of  $\pi \mu\text{m}^2$ . Four base current steps are shown:  $I_B=500, 600, 700,$  and  $800 \mu\text{A}$ .

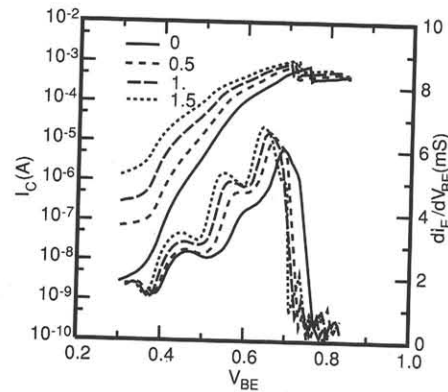


Fig.4 Dependence of collector current and input conductance,  $dI_E/dV_{BE}$ , on  $V_{BE}$  for the 40 nm base RHET at 4.2 K. Same device as in Fig.3.

conductance, are plotted as a function of  $V_{BE}$  for four values of collector/base voltage. Clear peaks in the conductance are observed with approximately 100 mV spacings. These are consistent with the calculated energy separations for the potential profile shown in Fig.1. The magnitude of the conductance oscillations increases with increasing collector/base bias which is consistent with an increase in the base transport factor due to more efficient

collection of electrons at the base/collector junction.

#### 4. MICROWAVE MEASUREMENTS

On-wafer s-parameter measurements were performed on the devices at room temperature using RF probes. The 10 nm base devices were not tested at microwave frequencies due to a fabrication problem. Shown in Fig.5 is the dependence of  $h_{21}$  and the maximum available gain (MAG) on frequency for the 40 nm base RHET. Extrapolating at -6 dB/octave, values for  $f_T=67$  GHz and  $f_{MAX}=41$  GHz are obtained.

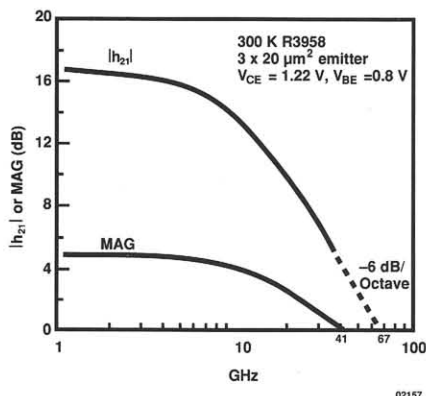


Fig.5. S-parameter measurements of the current gain,  $h_{21}$ , and maximum available gain (MAG) as a function of frequency.

Measurements of the 60 nm RHET were also obtained yielding an  $f_T$  of 54 GHz and an  $f_{MAX}$  of 11 GHz. Lower  $f_T$  in the wider base RHET is attributed to a decrease in the base transport factor. The MAG we observe in these RHETs could be further increased by reducing the base/collector leakage current which would in turn increase the output impedance of the transistor.

#### 5. CONCLUSIONS

We report the first room temperature InP-based hot electron transistors to exhibit dc gain greater than 10 and the

highest room temperature microwave gain yet achieved in the HET family. Room temperature operation is attributed to the notched RTD injector which lowers the energy of hot electrons injected into the base and thereby reduces intervalley transfer.

#### ACKNOWLEDGEMENTS

We would like to acknowledge many useful discussions with R.Bate, H.-Y.Liu, J.Luscombe, and M.Reed and the contract support of ONR/DARPA N00014-87-C-0363. Thanks also for the excellent technical assistance of P.Stickney, R.Thomason, B.Haven, B.Garmon, P.Williams, and F.Goodwin, and editorial assistance of R.Aggarwal.

#### REFERENCES

- 1) N.Yokoyama, K.Imamura, H.Ohnishi, T.Mori, and A.Shibatomi; Solid State Electron.31 (1988) 577.
- 2) T.Mori, K.Imamura, H.Ohnishi, Y.Minami, S.Muto, and N.Yokoyama, Conf.SSDM(1988)507.
- 3) A.F.J.Levi and T.H.Chiu, Appl.Phys.Lett. 51(1987) 985.
- 4) T.P.E.Broekaert, W.Lee, and C.G.Fonstad; Appl.Phys.Lett.53(1988) 1545.
- 5) J.Luscombe and W.Frensley; submitted to Nanotechnology.
- 6) M.Heiblum, M.V.Fischetti, W.P.Dumke, D.J.Frank, I.M.Anderson, C.M.Knoedler, and L.Osterling; Phys.Rev.58(1987) 816.